AGU PUBLICATIONS

Geophysical Research Letters

RESEARCH LETTER

10.1002/2015GL066615

Key Points:
- Many observationally constrained data sets of daily precipitation exist
- We highlight a large discrepancy in mean daily precipitation intensity between these data sets
- Thus, users should not treat all observational data sets of precipitation equally

Supporting Information:
- Text S1, Figures S1–S3, and Caption of Table S1
- Table S1

Correspondence to:
N. Herold,
nicholas.herold@unsw.edu.au

Citation:
Herold, N., L. V. Alexander, M. G. Donat, S. Contractor, and A. Becker (2016), How much does it rain over land?, *Geophys. Res. Lett.*, *43*, 341–348, doi:10.1002/2015GL066615.

Received 21 OCT 2015
Accepted 25 NOV 2015
Accepted article online 1 DEC 2015
Published online 9 JAN 2016

How much does it rain over land?

N. Herold[1], L. V. Alexander[1], M. G. Donat[1], S. Contractor[1], and A. Becker[2]

[1]Climate Change Research Centre and ARC Centre of Excellence for Climate System Science, University of New South Wales, Sydney, New South Wales, Australia, [2]Global Precipitation Climatology Centre, Deutscher Wetterdienst, Offenbach am Main, Germany

Abstract Despite the availability of several observationally constrained data sets of daily precipitation based on rain gauge measurements, remote sensing, and/or reanalyses, we demonstrate a large disparity in the quasi-global land mean of daily precipitation intensity. Surprisingly, the magnitude of this spread is similar to that found in the Coupled Model Intercomparison Project Phase 5 (CMIP5). A weakness of reanalyses and CMIP5 models is their tendency to over simulate wet days, consistent with previous studies. However, there is no clear agreement within and between rain gauge and remotely sensed data sets either. This large discrepancy highlights a shortcoming in our ability to characterize not only modeled daily precipitation intensities but even observed precipitation intensities. This shortcoming is partially reconciled by an appreciation of the different spatial scales represented in gridded data sets of in situ precipitation intensities and intensities calculated from gridded precipitation. Unfortunately, the spread in intensities remains large enough to prevent us from satisfactorily determining how much it rains over land.

1. Introduction

Predicting trends in precipitation intensity due to climate change is of significant societal and economic importance [*Arent et al.*, 2014]. Long-term, high-quality daily precipitation data sets are crucial for assessing these trends as well as for conducting detection and attribution studies. Over the past decade several quasi-global and global data sets of daily precipitation—and indices calculated from daily precipitation—have been developed, drawing from growing networks of rain gauges as well as remote sensing instruments [*Huffman et al.*, 2009; *Chen et al.*, 2008; *Menne et al.*, 2012; *Funk et al.*, 2013; *Donat et al.*, 2013a, 2013b]. These data sets have been of great utility to the climate extremes community in understanding the changing frequency, intensity, and duration of extreme precipitation events, for evaluating climate models, and for teasing apart the anthropogenic influence on climate extremes [e.g., *Min et al.*, 2011; *Sillmann et al.*, 2013].

However, data sets of observable quantities such as precipitation are often treated equally and without appropriate consideration of their differences. Numerous issues exist in creating globally gridded data sets from observations that can influence actual values of precipitation as well as temporal and spatial trends. In addition to issues of quality control, instrument choice and calibration, and the digitization of measurements, methodological issues exist in the interpolation of point data onto a global grid. The most common of these issues includes order of operations (i.e., scaling), choice of interpolation scheme, and the handling of missing data [e.g., *Hofstra et al.*, 2008, 2010; *Donat et al.*, 2014; *Dunn et al.*, 2014; *Gervais et al.*, 2014; *Avila et al.*, 2015].

In addition to gridded data sets based on gauge measurements and remotely sensed data, reanalyses provide global model-predicted but observationally constrained precipitation data over the satellite era and earlier, extending the spatial and temporal range over which trends in the climate system can be assessed. The latest iteration of the Coupled Model Intercomparison Project (CMIP5) provides a means for extending this coverage forward in time. Observational data sets, reanalyses, and CMIP5 simulations have all been used in one form or another to assess changes in precipitation extremes [e.g., *Sillmann et al.*, 2013; *Donat et al.*, 2014].

In this paper we show that a substantial disparity exists in a simple index of daily precipitation intensity within and between observational and reanalysis products. Further, we show that the spread between these products is as large as that exhibited by CMIP5 models. While it may not be surprising that unconstrained CMIP5 simulations exhibit large differences, the lack of consistency within and between observationally constrained products suggests that while we may lament the dreary state of precipitation in models,

Table 1. Observational and Reanalysis Products

Data Set	Temporal Coverage	Resolution	Instruments/Assimilation	1979–2005 Trend[a] (mm/d/decade)	Reference
			Observations		
HadEX2	1901–2010	3.75° × 2.5°	Gauge	3.5×10^{-4}	*Donat et al.* [2013b]
GHCNDEX-merged	1901 to present	3.75° × 2.5°	Gauge	-4.6×10^{-4}	*Dittus et al.* [2015]
CPC	1979–2005	0.5° × 0.5°	Gauge	3.0×10^{-4}	*Chen et al.* [2008]
GPCP-1DD	1997–2014	1° × 1°	Satellite, gauge adjusted.	NA[b]	*Huffman et al.* [2001]
GPCC-FDD	1988–2013	1° × 1°	Gauge	$\mathbf{1.5 \times 10^{-3}}$	*Schamm et al.* [2015]
			Reanalyses		
NCEP	1948–2012	1.875° × ~1.9°, 28 levels	3D-VAR	$\mathbf{5.1 \times 10^{-4}}$	*Kalnay et al.* [1996]
NCEP2	1979–2012	1.875° × ~1.9°, 28 levels	3D-VAR	7.6×10^{-5}	*Kanamitsu et al.* [2002]
ERA40	1958–2001	1.125° × ~1.125°, 60 levels	3D-VAR	$\mathbf{1.6 \times 10^{-3}}$	*Uppala et al.* [2005]
ERA-int	1979–2012	0.7° × ~0.7°, 60 levels	4D-VAR	3.1×10^{-4}	*Dee et al.* [2011]
JRA-55	1959–2013	0.55° × ~0.55°, 60 levels	4D-VAR	1.6×10^{-4}	*Kobayashi et al.* [2015]
20CR	1900–2010	1.875° × ~1.9°, 28 levels	Ensemble Kalman filter	7.4×10^{-5}	*Compo et al.* [2011]

[a]Sen's slope estimator. Bold indicates significance at the 5% level using the Mann-Kendall test. GPCC-FDD trend from 1988.
[b]Not Applicable.

as *Stephens et al*. [2010] did, we should be equally concerned with our ability to characterize precipitation from observations, without which we cannot reliably evaluate models to begin with. Discussion of the interpretation of observational products provides a means by which the discrepancies shown here may be better taken into account.

2. Data and Methods

We examine several observational, reanalysis, and CMIP5 products, which are summarized in Table 1 (Table S1 in the supporting information for CMIP5). HadEX2 is a quasi-global, gridded land-based data set of climate extremes indices developed by the Expert Team on Climate Change Detection and Indices (ETCCDI) [*Zhang et al*., 2011] and is based on numerous official rain gauge networks as well as data sourced from regional collaborations [*Donat et al*., 2013b]. Each precipitation index is calculated at rain gauge locations and interpolated onto a global grid using a modified form of angular distance weighting. To interpolate data to a grid cell, in situ data from locations within a gauge-dependent decorrelation length scale are used. Because of this, grid cells with no in situ data within the radius of the corresponding decorrelation length scale do not contain any interpolated values. The Global Historical Climatology Network's (GHCN's) daily precipitation data set is a rain gauge product that covers a substantial amount of the global land surface [*Menne et al*., 2012] and is largely independent of the rain gauge networks used in HadEX2. It has been used to create a structurally similar gridded extremes indices data set, designated GHCNDEX [*Donat et al*., 2013a]. This product utilizes only publicly available data; thus, due to restrictions on the availability of some data GHCNDEX lacks temporal coverage in crucial regions where data exist, such as the Indian subcontinent. To take advantage of GHCNDEX but alleviate data gaps, we use a merged product (GHCNDEX-merged) that supplements GHCNDEX with HadEX2 where data in the former are missing [*Dittus et al*., 2015]. The Climate Prediction Center's (CPC's) global daily precipitation data set is a new high-density 0.5° gridded rain gauge product built with optimal interpolation and adjusted for topographic biases [*Chen et al*., 2008]. This product covers the period 1979–2005. The Global Precipitation Climatology Project's 1° daily data set (GPCP-1DD) is a merged product of satellite infrared and microwave measurements that has been scaled to the GPCP version 2 monthly satellite-gauge data set, ensuring monthly precipitation totals of daily precipitation are consistent with this more robust data set [*Huffman et al*., 2001]. GPCP-1DD utilizes different remote sensing products poleward of 40°, and thus, artifacts can often be observed at this latitude. While monthly precipitation is relatively robust, the authors of this product note that given assumptions in the determination of rainfall and its distribution at submonthly time scales, daily values should be used cautiously [*Huffman et al*., 2001]. Further, while GPCP-1DD has global spatial coverage it is limited to post October 1996. Finally, the Global Precipitation Climatology Centre's (GPCC's) Full Data Daily product (GPCC-FDD) has been included [*Schamm et al*., 2015]. GPCC-FDD is a combination of in situ data from the Global Telecommunication System and other global and regional data collections that has been interpolated using kriging to a 1° grid. GPCC-FDD covers the period 1988 to 2013. Other data sets of daily or subdaily precipitation exist that are not included here.

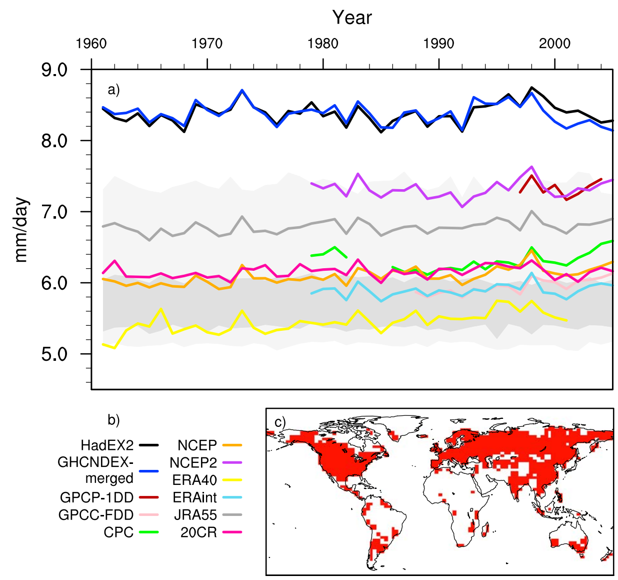

Figure 1. (a) Simple daily intensity index (SDII) for the period 1961–2005; (b) observations and reanalyses assessed in this paper. Light and dark grey shading represents the full and interquartile range of CMIP5 simulations (Table S1), respectively. (c) Region mask where satisfactory data coverage exists in all products (see text) and over which SDII is averaged.

For example, the Climate Hazards Group InfraRed Precipitation with Station data has released a new extremely high-resolution ($0.05 \times 0.05°$) gridded daily product [*Funk et al.*, 2013]. Unfortunately, this product lacks coverage poleward of 50° (i.e., much of Russia, northern Europe, and Canada) and is thus excluded. For similar reasons, the remotely sensed Tropical Rainfall Measuring Mission T3B42 product [*Huffman et al.*, 2007] and Precipitation Estimation from Remotely Sensed Information using Artificial Neural Networks-Climate Data Record product [PERSIANN-CDR; *Ashouri et al.*, 2014] are also excluded. For a separate analysis of tropical and subtropical regions including these products, refer to the supporting information. This additional analysis does not affect our conclusions. In addition to observational data sets, we examine most of the major reanalyses as well as output from historical simulations from the CMIP5 archive. The CMIP5 simulations used here represent a single ensemble member from each corresponding model and are taken from *Sillmann et al.* [2013]. Given the limited temporal coverage of the products considered here, we limit our study to the period 1961–2005.

We compare all data sets using the Simple Daily Intensity Index (SDII) as recommended by the ETCCDI. The R package climdex.pcic, developed by the Pacific Climate Impacts Consortium, was used for this process as it is considered the official implementation of the ETCCDI indices. SDII is an annual index defined as

$$\mathrm{SDII} = \frac{\sum \text{precipitation for days} \geq 1\,\text{mm}}{\text{number of days with precipitation} \geq 1\,\text{mm}} \tag{1}$$

SDII was calculated for all data sets at their native resolution and regridded to the HadEX2 grid ($3.75 \times 2.5°$) for comparison, using a second-order conservative interpolation scheme [*Jones*, 1999]. The ETCCDI has strict data completeness requirements that were adhered to in this study. Namely, at any grid cell no more than three daily values may be missing in any 1 month; otherwise, the entire month is considered missing. Similarly, no more than 15 days in any year may be missing; otherwise, the entire year is considered missing. This is done to limit spurious temporal trends. We further apply a single mask to all data sets requiring SDII values for at least 70% of the 1961–2005 period and at least 3 of the first and last 10 years, in each grid cell and for each product (Figure 1c). This latter step ensures that all products are assessed with the same spatial coverage but unfortunately also means that this spatial coverage is substantially less than global. Finally, years that did not have at least 80% spatial coverage of the masked area were removed to prevent large regional biases from influencing trends (e.g. as seen in Figure 1, CPC, between 1983 and 1985).

3. Results

Throughout the text we refer to data sets constructed from rain gauge and remotely sensed measurements as "observations," reanalysis products as "reanalyses," and CMIP5 simulations as "CMIP5." The mean SDII time series calculated for each data set reveals a substantial and persistent spread throughout 1961–2005, from ~5.2 mm/d in CMIP5 to ~8.4 mm/d in HadEX2 and GHCNDEX-merged (Figure 1). Substantial spread also exists within and between observational, reanalysis, and CMIP5 products. This result is robust to changes in our data mask, with similarly disparate values obtained using unmasked global land means (Figure S1).

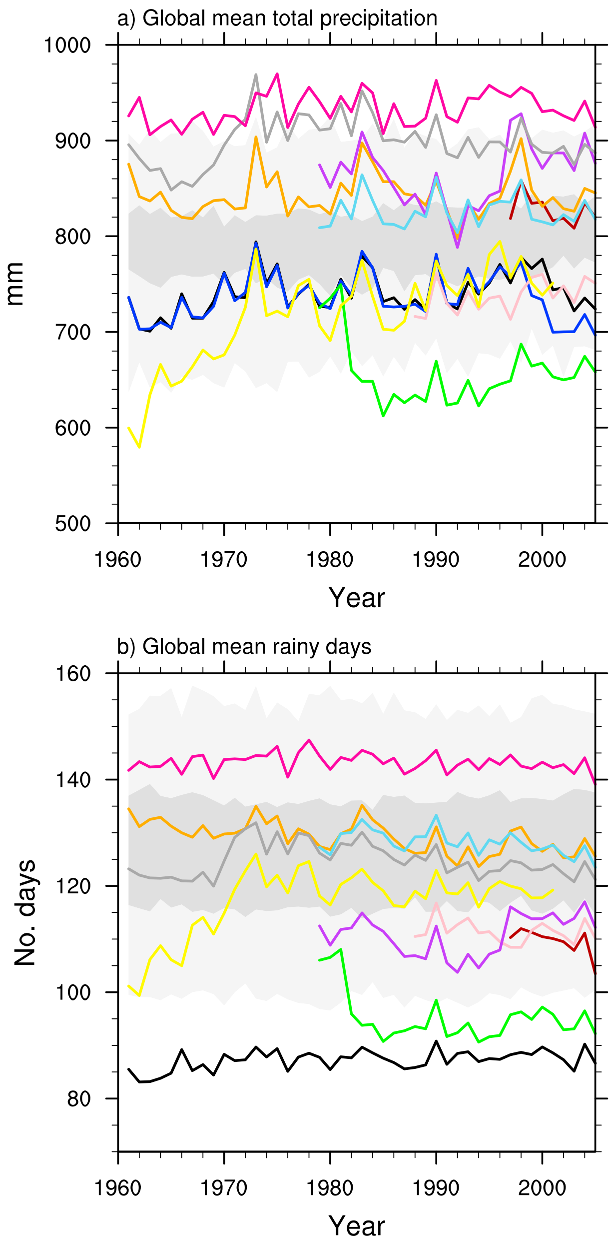

Figure 2. (a) Total precipitation and (b) number of wet days (days experiencing ≥ 1 mm) averaged over the regions indicated in Figure 1c. Legend as in Figure 1. Light and dark grey shading represent the full and interquartile ranges of CMIP5 simulations (Table S1), respectively. Given limits on the public availability of the raw data used in HadEX2, the total precipitation index developed by the ETCCDI [*Donat et al.*, 2013b] was combined with SDII to calculate the number of wet days for this data set. This could not be achieved with GHCNDEX-merged given that grid cells contributed by GHCNDEX and HadEX2 are not identical between SDII and the total precipitation index.

Of the observational data sets HadEX2 and GHCNDEX-merged exhibit the highest mean precipitation intensities (~8.4 mm/d) and GPCC-FDD the lowest (~5.9 mm/d). GHCNDEX-merged and HadEX2 closely resemble each other, and similarly, though to a lesser extent, so do CPC and GPCC-FDD. Both of these similarities are expected given that HadEX2 and GHCNDEX-merged—in addition to the former supplementing the latter—derive SDII from raw gauge data that is subsequently gridded, while CPC and GPCC-FDD derive SDII from raw gauge data that has already been gridded. The latter order of operations is known to produce lower values due to the averaging down of local maxima and the artificial increase in precipitation frequency [*Avila et al.*, 2015; *Donat et al.*, 2014; *Kursinski and Zeng*, 2006]. Mean intensity in GPCP-1DD—the only product with precipitation derived from satellite measurements—lies midway between the above pairs of data sets, at ~7.3 mm/d (Figure 1). The inclusion of observational products covering only tropical and subtropical regions does not alter our conclusions and in fact increases the spread in precipitation intensities that would otherwise exist (Figure S2 and supporting information).

To investigate interproduct variation, we examine the two components of SDII (equation (1)): the global mean (masked) total precipitation and number of wet days. Raw data for HadEX2 are unavailable; however, the total precipitation index developed by the ETCCDI is available as part of this data set [*Donat et al.*, 2013b], and combined with SDII can be used to calculate the number of wet days. The same could not be achieved with GHCNDEX-merged given that grid cells contributed by GHCNDEX and HadEX2 are not identical between SDII and the total precipitation index. Consequently, the number of wet days is not plotted for GHCNDEX-merged (Figure 2b). Of the observational data sets, HadEX2, GHCNDEX-merged, and GPCC-FDD produce very similar precipitation totals for overlapping years, while CPC produces precipitation totals substantially lower and GPCP-1DD substantially higher (Figure 2a). Conversely, HadEX2 and CPC produce a similar number of wet days for most of the period, while GPCP-1DD and GPCC-FDD produce higher values (Figure 2b). A large decrease in total precipitation and number of wet days occurs in CPC between 1981 and 1982 (Figure 2), before which CPC exhibits wet days consistent with

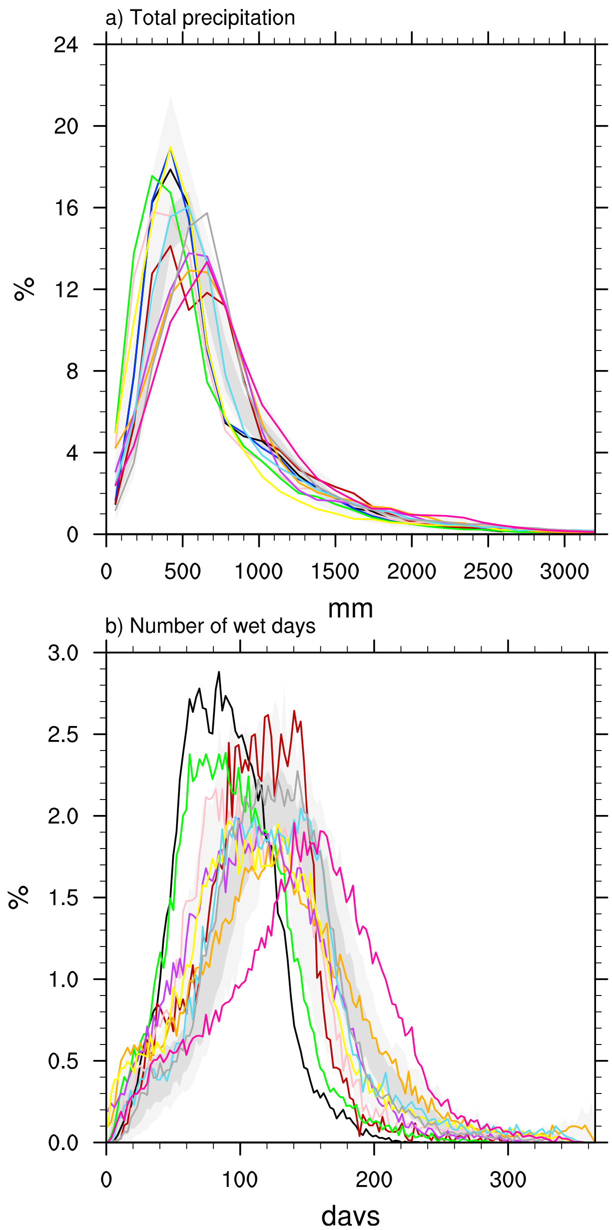

Figure 3. Probability distribution of (a) total precipitation and (b) the number of wet days, averaged over the regions indicated in Figure 1c. Legend as in Figure 1. Light and dark grey shadings represent the full and interquartile ranges of CMIP5 simulations (Table S1), respectively. GHCNDEX-merged not included in wet day calculation as per Figure 2.

the later GPCP-1DD and GPCC-FDD records. This decrease results from an ostensible inhomogeneity in precipitation across northern Eurasia. However, SDII is robust to these changes given their ratio remains comparatively constant.

Of the reanalyses NCEP2 exhibits the highest SDII and along with JRA55 is consistent with the brief GPCP-1DD record over our masked region (~7.3 mm/d; Figure 1). The remaining reanalyses fall closer to CPC and GPCC-FDD, although ERA40 exhibits intensities lower than all observational data sets and toward the lower end of CMIP5 simulations (Figure 1). NCEP2 acquires its high-precipitation intensity compared to other reanalyses due primarily to fewer simulated wet days, which is also more consistent with observations (Figure 2b). Conversely, ERA40 attains its low intensities compared to other reanalyses due to substantially lower precipitation totals (~50 mm lower than other reanalyses at the end of the period; Figure 2a). A large increase in total annual precipitation and number of rainy days prior to 1973 in ERA40 (Figure 2) results from strong precipitation trends over North America and Europe (not shown) and coincides with the beginning of satellite data assimilation in this product [*Uppala et al.*, 2005]. The spread in SDII between CMIP5 models is slightly larger than that between reanalyses, though with a clear tendency toward lower intensities (Figure 1). This is due predominantly to lower precipitation totals as opposed to a higher number of wet days (Figure 2). Exceptions are the MPI-ESM-MR, MPI-ESM-LR, and CMCC-CM models which constitute the large upper quartile extent of CMIP5 (Figure 1).

The data assimilation applied in reanalyses leads to distinct El Niño (e.g., 72–73, 82–83, and 97–98) and La Niña events (e.g., 88–89), manifesting themselves in increases and decreases in precipitation intensity, respectively (Figure 1). The sign of this response is a result of our data mask (Figure 1c) which favors the North American teleconnection to the tropical Pacific Ocean. 20CR captures these El Niño and La Niña events less well compared to other reanalyses and in particular over predicts wet days (Figure 3b), mainly over North America, northern Europe, and China (Figure S2). This deviation from other reanalyses is likely due to 20CR's assimilation of sea level pressure alone, which was done in order to limit inhomogeneities resulting from multiple observing systems and a long operational period [*Compo et al.*, 2011].

The differences between gauge-based data sets and the satellite-based GPCP-1DD, reanalyses, and CMIP5 are visible in the probability distributions for total precipitation and number of wet days (Figure 3), with the former exhibiting slightly more low precipitation totals and fewer wet days. While probability distributions of total precipitation and wet day frequency are generally consistent among reanalyses, 20CR substantially over simulates the frequency of wet days (Figure 3b). The spatial pattern of the mean total precipitation and number of wet days is similar among the observational and reanalysis products, though the magnitudes vary considerably (Figure S3). Compared to observations, all reanalyses rain too frequently in southern China and to varying degrees in eastern North America (Figure S3b).

Despite the large discrepancies in precipitation intensity, the 1979–2005 trends from observational and reanalysis data sets—except for GHCNDEX-merged and GPCP-1DD (for which the record is too short for trend analysis)—are all weakly positive, though most of these trends are not statistically significant (Table 1). Surprisingly, trends from CMIP5 exhibit little agreement with observations and reanalyses; with only 5 of the 28 simulations showing a positive trend, none of which are significant. Thus, for the regions considered here (Figure 1c) the trend in daily precipitation intensity seems robust to differences in gridding technique, order of operations, and whether model-derived or purely observational data are used, although data assimilation seems necessary for modeling to achieve the observed trend.

4. Discussion and Conclusion

A simple precipitation intensity index, SDII, varies substantially between observational, reanalysis, and CMIP5 products over the period 1961–2005. While the inherent spatial scale of model and remotely sensed data differs from the in situ information provided by rain gauges (i.e., HadEX2, GHCNDEX-merged, CPC, and GPCC-FDD), the spread within the different product types are themselves large.

HadEX2 and GHCNDEX-merged exhibit the highest precipitation intensities of all data sets due primarily—in the case of HadEX2—to their depiction of fewer wet days (Figures 2b and 3b). Both data sets exhibit intensities well above the range of CMIP5 simulations as well as reanalyses. While *Mehran et al*. [2014] found that CMIP5 models predict monthly precipitation totals well compared to GPCP measurements—consistent with our comparison (Figure 2a)—it is well documented that models tend to over predict precipitation frequency and under predict intensity compared to observations [*Dai and Trenberth*, 2004; *Sun et al*., 2007; *Stephens et al*., 2010], as reflected in Figures 1, 2b, and 3b. *Sillmann et al*. [2013] were the first to note a substantial under prediction of SDII in CMIP5 models compared to HadEX2. However, their choice of HadEX2 may not have been, as they acknowledge, the most appropriate for evaluating precipitation extremes in climate models given the order of operations used in HadEX2's construction [*Donat et al*., 2013b].

Which observational product a user should adopt in their research is not a trivial choice. Using HadEX2 versus GPCC-FDD, for example, could lead to wildly different results if actual values—as opposed to anomalies or trends—are of concern (Figure 1). Furthermore, the lack of guidance in the literature limits users' confidence in making such decisions. While data quality and spatial/temporal coverage are significant factors to consider, a less noted distinction between data sets are the spatial scales that they most appropriately represent. Recalling the message from *Chen and Knutson* [2008] that model simulated precipitation should be interpreted as an area average, researchers evaluating model results should then endeavor to use data sets best representing area averages, as opposed to in situ values. Results from previous studies suggest that differences in orders of operation may have contributed substantially to the spread in precipitation intensities seen here [*Avila et al*., 2015; *Donat et al*., 2014; *Dunn et al*., 2014; *Kursinski and Zeng*, 2006]. HadEX2 and GHCNDEX-merged, both constructed from gauge-based SDII that are subsequently gridded, exhibit mean precipitation intensities ~2.4 mm/d above CPC and GPCC-FDD, which calculate SDII from gridded gauge-based precipitation. Given the order of operations used in constructing these data sets, CPC and GPCC-FDD better reflect area-averaged precipitation intensity compared to HadEX2 and GHCNDEX-merged and on this basis may constitute more appropriate choices for model evaluation. GPCP-1DD, a satellite product derived inherently from area averages, also provides an appropriate comparison to model data. While precipitation intensity from CPC and GPCC-FDD compares more closely to reanalyses and CMIP5 than GPCP-1DD (Figure 1), this is belied by the fact that both data sets exhibit substantially lower precipitation totals than most models (Figure 2a). It is also worth noting here that gauge density varies greatly between grid cells and can severely affect the accuracy of the estimated precipitation intensity. *Kursinski and Zeng* [2006] show that for a midlatitude region in the United States, approximately 30 gauge stations are required to accurately estimate precipitation intensity within a 200×200 km area. This level of data coverage can only be expected over some regions and only in developed countries; thus, further bias may exist in the gauge-based products assessed here where the number of gauges is substantially lower than this. GPCP-1DD, on the other hand, relies on approximations of precipitation from measurements of cloud top temperatures and makes assumptions about the daily intensity of precipitation within any given month. Ultimately, there is no objective way of knowing whether gridded gauge data or satellite data more accurately reflect area-averaged precipitation intensity. It is clear that the former may become increasingly biased as the number of stations available for interpolation decreases [e.g., *Hofstra et al.*, 2010; *Gervais et al.*, 2014; *Kursinski and Zeng*, 2006] and that the latter depends on indirect methods, measuring radiation quantities related to precipitation through empirical relationships which vary in efficacy by region.

Users with an interest in site-specific precipitation intensity should, conversely, select data sets best representing in situ values, which in this case are HadEX2 and GHCNDEX-merged. It is arguable that the in situ values used in constructing HadEX2 and GHCNDEX-merged are the only precipitation intensities of physical relevance, as they are recorded intensities as opposed to derivations from approximated area averages. Nonetheless, area averages of climate variables form the basis for climate model evaluation, and thus, data sets representing these averages are necessary. On this basis, it may be unreasonable to expect agreement between HadEX2 and GHCNDEX-merged, and GPCC-FDD and CPC. When considering only GPCC-FDD, CPC, and GPCP-1DD, climate models have a narrower observational range at which to aim for, and in fact, many reanalyses and some CMIP5 models already achieve this target (Figure 1). Though, by all observational accounts, most models still oversimulate wet day frequency (Figure 2b) and thus generally underestimate precipitation intensity (Figure 1).

The most salient result of this study is that differences in precipitation intensity among observational datasets are as large as those among reanalyses or among CMIP5 models (~2.4 mm/d; Figure 1). Given the increasing importance and availability of daily precipitation data sets for monitoring climate change, it is necessary that their differences are considered when used. It is frequently reported that climate models precipitate too frequently and/or not intensely enough [*Dai and Trenberth*, 2004; *Sun et al.*, 2007; *Stephens et al.*, 2010]. While these are legitimate concerns, our results suggest that how well a model evaluates may depend strongly on the observational data set used if actual amounts are of concern. The quality and density of data coverage varies by region, and the data set against which to evaluate models should thus vary accordingly. Nevertheless, the trends in the data sets assessed here are robust, and thus, our results do not diminish their utility in projecting rates of change or determining spatial patterns. Ultimately, the data set adopted for a particular problem must be “fit for purpose” and requires substantial user discretion.

Acknowledgments
This work contributes to the WCRP Grand Challenge on Extremes. N.H., L.V.A., and S. C. were funded through ARC grant CE110001028. M.G.D. was funded through ARC grant DE150100456. We acknowledge the World Climate Research Programme’s Working Group on Coupled Modelling, which is responsible for CMIP, and we thank the climate modeling groups (listed in Table S1 of this paper) for producing and making available their model output. For CMIP the U.S. Department of Energy’s Program for Climate Model Diagnosis and Intercomparison provides coordinating support and led development of software infrastructure in partnership with the Global Organization for Earth System Science Portals. NCEP Reanalysis 1 and 2 data provided by the NOAA/OAR/ESRL PSD, Boulder, Colorado, USA, from their website at http://www.esrl.noaa.gov/psd/. JRA-55: Japanese 55 year Reanalysis, daily 3 hourly and 6 hourly data provided by Research Data Archive at the National Center for Atmospheric Research, Computational and Information Systems Laboratory. Data are processed with the Climate Data Operators. Plots are created with the NCAR Command Language [http://dx.doi.org/10.5065/D6WD3XH5]. We thank Ali Behrangi for help in obtaining satellite data.

References

Arent, D. J., R. S. J. Tol, E. Faust, J. P. Hella, S. Kumar, K. M. Strzepek, F. L. Tóth, and D. Yan (2014), Key economic sectors and services, in *Climate Change 2014: Impacts, Adaptation, and Vulnerability. Part A: Global and Sectoral Aspects. Contribution of Working Group II to the Fifth Assessment Report of the Intergovernmental Panel of Climate Change*, edited by C. B. Field et al., pp. 659–708, Cambridge Univ. Press, Cambridge, U. K., and New York.

Ashouri, H., K.-L. Hsu, S. Sorooshian, D. K. Braithwaite, K. R. Knapp, L. D. Cecil, B. R. Nelson, and O. P. Prat (2014), PERSIANN-CDR: Daily precipitation climate data record from multisatellite observations for hydrological and climate studies, *Bull. Am. Meteorol. Soc.*, *96*(1), 69–83, doi:10.1175/BAMS-D-13-00068.1.

Avila, F. B., S. Dong, K. P. Menang, J. Rajczak, M. Renom, M. G. Donat, and L. V. Alexander (2015), Systematic investigation of gridding-related scaling effects on annual statistics of daily temperature and precipitation maxima: A case study for south-east Australia, *Weather Clim. Extremes*, *9*, 6–16, doi:10.1016/j.wace.2015.06.003.

Chen, C.-T., and T. Knutson (2008), On the verification and comparison of extreme rainfall indices from climate models, *J. Clim.*, *21*(7), 1605–1621, doi:10.1175/2007JCLI1494.1.

Chen, M., P. Xie, and Co-authors (2008), CPC Unified Gauge-based Analysis of Global Daily Precipitation, paper presented Western Pacific Geophysics Meeting, Cairns, Australia, 29 July – 1 Aug.

Compo, G. P., et al. (2011), The twentieth century reanalysis project, *Q. J. R. Meteorol. Soc.*, *137*(654), 1–28, doi:10.1002/qj.776.

Dai, A., and K. E. Trenberth (2004), The diurnal cycle and its depiction in the community climate system model, *J. Clim.*, *17*(5), 930–951, doi:10.1175/1520-0442(2004)017<0930:TDCAID>2.0.CO;2.

Dee, D. P., et al. (2011), The ERA-Interim reanalysis: Configuration and performance of the data assimilation system, *Q. J. R. Meteorol. Soc.*, *137*(656), 553–597, doi:10.1002/qj.828.

Dittus, A. J., D. J. Karoly, S. C. Lewis, and L. V. Alexander (2015), A multi-region assessment of observed changes in the areal extent of temperature and precipitation extremes, *J. Clim.*, *28*(23), 9206–9220, doi:10.1175/JCLI-D-14-00753.1.

Donat, M. G., L. V. Alexander, H. Yang, I. Durre, R. Vose, and J. Caesar (2013a), Global land-based datasets for monitoring climatic extremes, *Bull. Am. Meteorol. Soc.*, *94*(7), 997–1006, doi:10.1175/BAMS-D-12-00109.1.

Donat, M. G., et al. (2013b), Updated analyses of temperature and precipitation extreme indices since the beginning of the twentieth century: The HadEX2 dataset, *J. Geophys. Res. Atmos.*, *118*, 2098–2118, doi:10.1002/jgrd.50150.

Donat, M. G., J. Sillmann, S. Wild, L. V. Alexander, T. Lippmann, and F. W. Zwiers (2014), Consistency of temperature and precipitation extremes across various global gridded in situ and reanalysis datasets, *J. Clim.*, *27*(13), 5019–5035, doi:10.1175/JCLI-D-13-00405.1.

Dunn, R. J. H., M. G. Donat, and L. V. Alexander (2014), Investigating uncertainties in global gridded datasets of climate extremes, *Clim. Past*, *10*(6), 2171–2199, doi:10.5194/cp-10-2171-2014.

Funk, C. C., P. J. Peterson, M. F. Landsfeld, D. H. Pedreros, J. P. Verdin, J. D. Rowland, B. E. Romero, G. J. Husak, J. C. Michaelsen, and A. P. Verdin (2013), A quasi-global precipitation time series for drought monitoring, *U.S. Geol. Surv. Data Ser.*, 832, 4, doi:10.3133/ds832.

Gervais, M., L. B. Tremblay, J. R. Gyakum, and E. Atallah (2014), Representing extremes in a daily gridded precipitation analysis over the United States: Impacts of station density, resolution, and gridding methods, *J. Clim.*, *27*(14), 5201–5218, doi:10.1175/JCLI-D-13-00319.1.

Hofstra, N., M. Haylock, M. New, P. Jones, and C. Frei (2008), Comparison of six methods for the interpolation of daily, European climate data, *J. Geophys. Res.*, *113*, D21110, doi:10.1029/2008JD010100.

Hofstra, N., M. New, and C. McSweeney (2010), The influence of interpolation and station network density on the distributions and trends of climate variables in gridded daily data, *Clim. Dyn.*, *35*(5), 841–858, doi:10.1007/s00382-009-0698-1.

Huffman, G. J., R. F. Adler, M. M. Morrissey, D. T. Bolvin, S. Curtis, R. Joyce, B. McGavock, and J. Susskind (2001), Global precipitation at one-degree daily resolution from multisatellite observations, *J. Hydrometeorol.*, *2*(1), 36–50, doi:10.1175/1525-7541(2001)002<0036:GPAODD>2.0.CO;2.

Huffman, G. J., D. T. Bolvin, E. J. Nelkin, D. B. Wolff, R. F. Adler, G. Gu, Y. Hong, K. P. Bowman, and E. F. Stocker (2007), The TRMM Multisatellite Precipitation Analysis (TMPA): Quasi-global, multiyear, combined-sensor precipitation estimates at fine scales, *J. Hydrometeorol.*, *8*(1), 38–55, doi:10.1175/JHM560.1.

Huffman, G. J., R. F. Adler, D. T. Bolvin, and G. Gu (2009), Improving the global precipitation record: GPCP version 2.1, *Geophys. Res. Lett.*, *36*, L17808, doi:10.1029/2009GL040000.

Jones, P. W. (1999), First- and second-order conservative remapping schemes for grids in spherical coordinates, *Mon. Weather Rev.*, *127*(9), 2204–2210, doi:10.1175/1520-0493(1999)127<2204:FASOCR>2.0.CO;2.

Kalnay, E., et al. (1996), The NCEP/NCAR 40-year reanalysis project, *Bull. Am. Meteorol. Soc.*, *77*(3), 437–471, doi:10.1175/1520-0477(1996)077<0437:TNYRP>2.0.CO;2.

Kanamitsu, M., W. Ebisuzaki, J. Woollen, S.-K. Yang, J. J. Hnilo, M. Fiorino, and G. L. Potter (2002), NCEP–DOE AMIP-II reanalysis (R-2), *Bull. Am. Meteorol. Soc.*, *83*(11), 1631–1643, doi:10.1175/BAMS-83-11-1631.

Kobayashi, S., et al. (2015), The JRA-55 Reanalysis: General specifications and basic characteristics, *J. Meteorol. Soc. Jpn.*, *93*, 5–48, doi:10.2151/jmsj.2015-001.

Kursinski, A. L., and X. Zeng (2006), Areal estimation of intensity and frequency of summertime precipitation over a midlatitude region, *Geophys. Res. Lett.*, *33*, L22401, doi:10.1029/2006GL027393.

Mehran, A., A. AghaKouchak, and T. J. Phillips (2014), Evaluation of CMIP5 continental precipitation simulations relative to satellite-based gauge-adjusted observations, *J. Geophys. Res. Atmos.*, *119*, 1695–1707, doi:10.1002/2013JD021152.

Menne, M. J., I. Durre, R. S. Vose, B. E. Gleason, and T. G. Houston (2012), An overview of the global historical climatology network-daily database, *J. Atmos. Oceanic Technol.*, *29*(7), 897–910, doi:10.1175/JTECH-D-11-00103.1.

Min, S.-K., X. Zhang, F. W. Zwiers, and G. C. Hegerl (2011), Human contribution to more-intense precipitation extremes, *Nature*, *470*(7334), 378–381.

Schamm, K., M. Ziese, K. Raykova, A. Becker, P. Finger, A. Meyer-Christoffer, and U. Schneider (2015), GPCC full data daily version 1.0 at 1.0°: Daily land-surface precipitation from rain-gauges built on GTS-based and historic data, doi:10.5676/DWD_GPCC/FD_D_V1_100.

Sillmann, J., V. V. Kharin, X. Zhang, F. W. Zwiers, and D. Bronaugh (2013), Climate extremes indices in the CMIP5 multimodel ensemble: Part 1. Model evaluation in the present climate, *J. Geophys. Res. Atmos.*, *118*, 1716–1733, doi:10.1002/jgrd.50203.

Stephens, G. L., T. L'Ecuyer, R. Forbes, A. Gettlemen, J.-C. Golaz, A. Bodas-Salcedo, K. Suzuki, P. Gabriel, and J. Haynes (2010), Dreary state of precipitation in global models, *J. Geophys. Res.*, *115*, D24211, doi:10.1029/2010JD014532.

Sun, Y., S. Solomon, A. Dai, and R. W. Portmann (2007), How often will it rain?, *J. Clim.*, *20*(19), 4801–4818, doi:10.1175/JCLI4263.1.

Uppala, S. M., et al. (2005), The ERA-40 re-analysis, *Q. J. R. Meteorol. Soc.*, *131*(612), 2961–3012, doi:10.1256/qj.04.176.

Zhang, X., L. Alexander, G. C. Hegerl, P. Jones, A. K. Tank, T. C. Peterson, B. Trewin, and F. W. Zwiers (2011), Indices for monitoring changes in extremes based on daily temperature and precipitation data, *Wiley Interdiscip. Rev. Clim. Change*, *2*(6), 851–870, doi:10.1002/wcc.147.